ARTICLE
Journal of Cellular Biochemistry 107:769–784 (2009)

Journal of Cellular Biochemistry

FGF-8b Induces Growth and Rich Vascularization in an Orthotopic PC-3 Model of Prostate Cancer

Maija P. Valta,[1,2*] Johanna Tuomela,[1,3] Heikki Vuorikoski,[1,3] Niina Loponen,[1] Riina-Minna Väänänen,[4] Kim Pettersson,[4] H. Kalervo Väänänen,[1] and Pirkko L. Härkönen[1,5]

[1]*Department of Cell Biology and Anatomy, Institute of Biomedicine, University of Turku, Turku, Finland*
[2]*Hospital District of Southwest Finland, Salo Regional Hospital, Internal Medicine, Salo, Finland*
[3]*Orthotopix Ltd, Turku, Finland*
[4]*Department of Biotechnology, University of Turku, Turku, Finland*
[5]*Department of Laboratory Medicine, Tumor Biology, MAS University Hospital, Lund University, Lund, Sweden*

ABSTRACT

Fibroblast growth factor 8 (FGF-8) is expressed at an increased level in a high proportion of prostate cancers and it is associated with a poor prognosis of the disease. Our aim was to study the effects of FGF-8b on proliferation of PC-3 prostate cancer cells and growth of PC-3 tumors, and to identify FGF-8b-associated molecular targets. Expression of ectopic FGF-8b in PC-3 cells caused a 1.5-fold increase in cell proliferation in vitro and a four- to fivefold increase in the size of subcutaneous and orthotopic prostate tumors in nude mice. Tumors expressing FGF-8b showed a characteristic morphology with a very rich network of capillaries. This was associated with increased spread of the cancer cells to the lungs as measured by RT-qPCR of FGF-8b mRNA. Microarray analyses revealed significantly altered, up- and downregulated, genes in PC-3 cell cultures (169 genes) and in orthotopic PC-3 tumors (61 genes). IPA network analysis of the upregulated genes showed the strongest association with development, cell proliferation (*CRIP1*, *SHC1*), angiogenesis (*CCL2*, *DDAH2*), bone metastasis (*SPP1*), cell-to-cell signaling and energy production, and the downregulated genes associated with differentiation (*DKK-1*, *VDR*) and cell death (*CYCS*). The changes in gene expression were confirmed by RT-qPCR. In conclusion, our results demonstrate that FGF-8b increases the growth and angiogenesis of orthotopic prostate tumors. The associated gene expression signature suggests potential mediators for FGF-8b actions on prostate cancer progression and metastasis. J. Cell. Biochem. 107: 769–784, 2009.

KEY WORDS: ANGIOGENESIS; FGF-8; GENE EXPRESSION; MICROARRAY; ORTHOTOPIC PROSTATE TUMORS; PROSTATE CANCER

Prostate cancer is among the most common malignancies of men in the world and its incidence is increasing [Parkin et al., 2001]. However, this can be partly explained by widespread screening and improved detection of indolent tumors [Parkin et al., 2001; Wilt and Thompson, 2006]. Prostate cancer is considered to arise from genetic changes disrupting homeostasis between the cells of prostate epithelial and stromal compartments. The molecular mechanisms behind the progression of prostate cancer to its life-threatening form are largely unknown. Recent data imply that fibroblast growth factors (FGFs) are involved in many of the

Abbreviations used: CCL2, small inducible cytokine A12; *CRIP1*, cystatin-related protein-1; *CYCS*, cytochrome *c*; *DDAH2*, dimethylarginine dimethylaminohydrolase 2; *DKK-1*, dickkopf-1; FGF, fibroblast growth factor; FGFR, fibroblast growth factor receptor; GO, Gene Ontology; H&E, hematoxylin–eosin; IPA, Ingenuity Pathways Analysis; MMP, matrix metalloproteinase; RT-PCR, reverse transcription polymerase chain reaction; RT-qPCR, quantitative reverse transcription, real-time polymerase chain reaction; sc, subcutaneous; *SHC1*, Src homology 2 domain containing transforming protein 1; *SPP1*, osteopontin; *VDR*, vitamin D receptor; VEGF, vascular endothelial growth factor.

Additional Supporting Information may be found in the online version of this article.

Grant sponsor: Academy of Finland; Grant sponsor: Finnish Cancer Societies; Grant sponsor: Sigrid Jusélius Foundation; Grant sponsor: Southwestern Finnish Cancer Societies; Grant sponsor: Finnish Cultural Foundation; Grant sponsor: European Union 6th Framework; Grant number: LSHC-CT-2004-503011.

*Correspondence to: Maija P. Valta, Department of Cell Biology and Anatomy, Institute of Biomedicine, University of Turku, Kiinamyllynkatu 10, FI-20520 Turku, Finland. E-mail: maija.valta@utu.fi

Received 9 August 2008; Accepted 17 March 2009 • DOI 10.1002/jcb.22175 • © 2009 Wiley-Liss, Inc.
Published online 4 May 2009 in Wiley InterScience (www.interscience.wiley.com).

reciprocal interactions of tumor cells and stromal cells that are affected in prostate tumorigenesis and cancer progression [Kwabi-Addo et al., 2004; Mattila and Harkonen, 2007; Zhang et al., 2008].

The human FGF family consists of 23 polypeptide growth factors that play important roles in many physiological and pathological processes including embryonic development, bone formation, angiogenesis and tumor growth [Powers et al., 2000]. At least FGF-1, FGF-2, FGF-6, FGF-8, FGF-9, and FGF-17 are known to be expressed at a high level in prostate cancer, where they function as paracrine and/or autocrine growth factors for prostate cancer cells [Valve et al., 2001; Heer et al., 2004; Kwabi-Addo et al., 2004; Li et al., 2008]. FGF-8 was originally cloned from Shionogi mouse mammary tumor-derived SC-3 cells [Tanaka et al., 1992]. Alternative splicing of the human FGF-8 gene allows transcription of four different isoforms designated FGF-8a, FGF-8b, FGF-8e, and FGF-8f [Ghosh et al., 1996]. FGF-8b is the major isoform expressed in prostate cancer and it correlates with the stage and grade of the disease [Gnanapragasam et al., 2003].

FGFs mediate their effects by binding to specific tyrosine kinase receptors (FGFR1–4) and to heparan sulfate proteoglycans with high affinity [Powers et al., 2000]. All four types of FGF receptor are expressed in prostate cancer at variable frequencies. FGF-8b is able to activate receptors slice forms FGFR1IIIc, FGFR2IIIc, FGFR3IIIc, and FGFR4 [MacArthur et al., 1995; Ornitz et al., 1996; Olsen et al., 2006]. The main intracellular pathways activated by FGF receptors are Ras-MAPK pathway, PI3K/Akt pathway and PLC-γ pathway [Dailey et al., 2005].

It has been suggested that FGF-8 is regulated by androgens in prostate cancer [Wang et al., 1999; Gnanapragasam et al., 2002]. Interestingly, there is also expression of FGF-8 in castration resistant prostate cancer [Dorkin et al., 1999]. Various immunohistochemical, mRNA and in situ hybridization analyses of clinical samples have shown increased expression of FGF-8 in prostate cancer epithelium but none or little in normal prostates [Tanaka et al., 1998; Dorkin et al., 1999; Valve et al., 2001]. Studies carried out in vitro and in vivo in experimental models have shown that FGF-8 increases growth, invasion and tumorigenesis of prostate cancer cells [Rudra-Ganguly et al., 1998; Song et al., 2000] and that FGF-8 targeted to prostate epithelium causes prostatic intraepithelial neoplasia in transgenic mice [Song et al., 2002]. Our previous studies have shown that FGF-8 is involved in prostate cancer bone metastasis [Valta et al., 2008], possibly via regulation of osteoblast differentiation [Valta et al., 2006, 2008], and in angiogenesis [Mattila et al., 2001; Aragon-Ching and Dahut, 2008], which is another critical step as regards prostate cancer growth.

The heterogeneous nature of prostate cancer hampers the prediction of clinical outcome. Studying molecular mechanisms behind the progression of prostate cancer may help to identify patients at a high risk of advanced disease. The aim of this study was to investigate the mechanisms by which FGF-8b influences prostate cancer progression. In order to mimic FGF-8b-expressing prostate tumors we used PC-3 cells ectopically expressing FGF-8b. The autocrine and paracrine gene targets of FGF-8b were sought by means of microarrays. Human and mouse microarrays were used to study changes in gene expression in human PC-3 tumor cells and in host-derived stromal cells in tumors, respectively. The analyses showed that FGF-8b induced distinct changes in gene expression profiles in PC-3 cells and orthotopic prostate tumors. These responses to FGF-8b may help in the search for new prognostic markers or anti-angiogenic therapeutic targets in prostate cancer.

MATERIALS AND METHODS

CELL CULTURE AND TRANSFECTION OF PC-3 CELLS WITH FGF-8b EXPRESSION VECTORS

Human prostate cancer cells (PC-3 cells) were obtained from American Type Culture Collection (ATCC, Rockville, MD). The cells were cultured using standard cell culture techniques and transfected with FGF-8b or empty vector (mock) cDNAs [Valta et al., 2008]. A clone expressing high amounts of FGF-8b (PC-3/FGF-8b clone 1, later called PC-3/FGF-8b), a moderately expressing clone (PC-3/FGF-8b clone 15) and a control clone (PC-3/mock) were selected for further tumor experiments.

RNA AND PROTEIN SAMPLING AND ANALYSIS

Total RNA was extracted from the cells using the guanidinium isothiocyanate method [Chirgwin et al., 1979] and from the tumor homogenates by using TRIZOL reagent (Invitrogen, Carlsbad, CA). Total RNA was subjected to Qiagen RNA cleanup (RNeasy Mini Kit, Qiagen, Germany) and DNaseI (Qiagen) treatment as described by the manufacturer. The quality of the RNAs was determined by spectrophotometry, on formaldehyde gels and with an Agilent 2100 Bioanalyzer (Agilent Technologies, USA), based on microfluidics technology of electrophoretic separation and fluorescence. Northern blotting, RT-PCR, and Southern blotting for FGFR1–4 were performed as previously described [Ruohola et al., 1995; Valta et al., 2006]. Western blotting for FGF-8b (anti-FGF-8b, R & D Systems, Minneapolis, MN) and FGFR2 antibody (C-17, Santa Cruz Biotechnology, Inc., CA) in the cells was performed as previously described [Ruohola et al., 2001].

ANALYSIS OF PC-3 CELL PROLIFERATION, MORPHOLOGY AND MMP PRODUCTION

For the proliferation study the cells were plated at a density of 40×10^3 cells/well in 24-well plates. Cell numbers were counted with a Coulter Counter (Coulter, Harpenden, UK) as previously described [Siren et al., 2004]. The morphology of the cells was analyzed by counting elongated cells per field of view in similarly confluent cell culture dishes or by measurement of cell length and breadth from magnified (200×) captured images (total of 100–300 cells in 4–6 different fields) using a Leica microscope and camera (Leitz Diavert, Germany). The data were histomorphometrically analyzed by using AxioVision Software (AxioVision Software, Carl Zeiss Microimaging GmbH, Oberkochen, Germany). Zymography to investigate the gelatinolytic activity of MMP was performed as previously described [Ruohola et al., 2001].

TUMOR EXPERIMENTS

The welfare of the mice (12-week-old male athymic nu/nu mice, Harlan, The Netherlands) was monitored daily and the animals were weighed once a week. The animal experiments were carried

out according to the European Convention for the Protection of Vertebrate Animals used for Experimental and other Scientific Purposes and Statutes 1076/85 § and 1360/90 of The Animal Protection Law in Finland and EU Directive 86/609. The experimental procedures were performed within the guidelines and with the approval of the University of Turku Ethics Committee and under the approval of state authorities. For the subcutaneous inoculations, 5×10^6 PC-3/FGF-8b or PC-3/mock cells were inoculated into the necks of mice (n = 30 and 22, respectively). For the orthotopic prostate inoculations, 5×10^5 cells were suspended in 20 μl of a sterile dye solution consisting of PBS with green dye (0.5 μg/ml; 33022 Roberts Oy, Turku, Finland). The mice were orthotopically inoculated with 5×10^5 PC-3/FGF-8b clone 1, PC-3/FGF-8b clone 15 or PC-3/mock cells into the ventral prostates of mice as previously described [Tuomela et al., 2008] (n = 12, 8, and 28, respectively). The success of inoculation was visualized by means of the dye added to the cell suspension.

HISTOLOGY AND IMMUNOHISTOCHEMISTRY

The mice were sacrificed 6 weeks after sc and 4 and 8 weeks after orthotopic cancer cell inoculation. Tumor volume was calculated according to Janik et al. [1975]. One-half of the tumor was then processed for histological examination and the other half was frozen for RNA analysis. Prostates, selected internal organs (lungs, spleen, liver, and kidneys), lymph nodes (iliac, sacral, inguinal, sciatic, axillary, and brachial) and bones (hind limbs and vertebrae) from orthotopically inoculated mice were immersed in 4% neutral-buffered formalin. Some of the subcutaneous tumors were frozen for immunohistological examination. The bones were subjected to radiography using a Faxitron MX-20 DC-2 X-ray cabinet (30 kVp, 6s, Faxitron X-ray Corp., IL). The tissue sections were stained with hematoxylin and eosin (H&E). The lymph nodes and internal organs were cut through collecting sections from 8 to 14 levels for analysis of the occurrence of metastases.

Orthotopic tumors were incubated with rat anti-CD34 (Santa Cruz Biotechnology, Inc.) and mouse anti-Ki67 (Novocastra, UK) antibodies overnight at +4°C. Biotin-labeled rabbit anti-rat IgG (DAKO Denmark A/S, Glostrup, Denmark) and goat anti-mouse IgG (Vector Laboratories, Burlingame, CO) were used as secondary antibodies. A Mouse-on-Mouse Kit (Vector Laboratories) was used for Ki67 antibody staining. Frozen tumor sections (10 μm) were fixed with 4% acetone for 10 min at +4°C and immunostained with rat anti-CD31 (PharMingen A Becton Dickinson Company) antibody overnight at +4°C. The samples were then treated with biotin-labeled rabbit anti-rat IgG (DAKO, Denmark A/S). Visualization of the primary antibody was carried out by using Vectastain ABC reagent and a diaminobenzidine substrate kit (Vector Laboratories). Negative controls (sections of every sample stained without the primary antibody) were used to verify the specificity of staining.

HISTOMORPHOMETRY

The relative areas of tumor metastases in iliac and sacral lymph nodes were histomorphometrically analyzed in H&E-stained sections (AxioVision Software, Carl Zeiss Microimaging GmbH). The numbers of Ki67-positive cells/field in multiple non-overlapping views of tumor area were counted using a high power microscope (200× magnification, Leica, DMRB, Leica Microsystems, Heerburg, Germany) and digital camera (Leica DC 300F, Leica Microsystems). The numbers of blood vessels of H&E-stained sections were counted. Vessels were counted if they were completely within the area of the graticule of the ocular grid or touched the top or left-hand border. Vessels touching the right-hand or bottom border were excluded. The vascular network in tumors was further analyzed by making use of the endothelial cell-specific antibodies CD34 (paraffin-embedded sections) and CD31 (frozen sections). The densities of CD34- and CD31-positive vessels were counted in three fields of each tumor as previously described [Tuomela et al., 2008], using Axiovision Software (AxioVision Software, Carl Zeiss Microimaging GmbH). All samples were analyzed in a blind fashion by two independent analyzers.

QUANTITATIVE RT-PCR (RT-qPCR) ANALYSIS FOR DETECTION OF METASTASIS

Lung, liver, and bone marrow samples for RT-qPCR were stored in RNAlater (Qiagen) and whole blood samples in PAXgene solution (PreAnalytix, Switzerland). Total RNA was extracted using an RNeasy Mini Kit (Qiagen) according to the manufacturer's instructions and a known amount of internal standard molecule [Nurmi et al., 2000] was added to each sample as RNA after cell lysis. RNA was transcribed into cDNA with a High Capacity cDNA Archive Kit (Applied Biosystems, Foster City, CA).

Polymerase chain reaction analyses were performed according to previously described protocols [Nurmi et al., 2000; Vaananen et al., 2008]. Briefly, RT-qPCR assays, with real-time detection based on time-resolved fluorescence, were used to determine both FGF-8b mRNA and internal standard RNA levels and original FGF-8b expression levels were calculated on the basis of these results. The oligonucleotides used (Thermo, Germany) are presented in Table I. The external standard curve consisted of three points between 1.3×10^2 and 1.3×10^5 molecules per milliliter and standards were prepared as previously described [Vaananen et al., 2008].

TABLE I. Oligonucleotides Used in FGF-8b RT-qPCR

Oligonucleotide	Sequence	Base positions
5′ Primer	5′-CTG CCT CCA AGC CCA GGT A-3′	224–242
3′ Primer	5′-CGG CTG AGC TGA TCC GTC A-3′	295–313
Reporter probe	5′-Tb-GCT CTG CTC CCT CAC ATG CTG TGT-3′	267–290
Quencher probe	5′-ATG TGA GGG AGC AGA GC-Dabcyl-3′	274–290

Bases denote the bases in database sequence NM_006119.

MICROARRAY HYBRIDIZATION AND DATA ACQUISITION

Agilent Human 1A (V2) oligomicroarrays containing 22,575 features were used for studying gene expression differences between PC-3/mock and PC-3/FGF-8b cells (Fig. 6a). Total RNA of separate samples was used for cDNA synthesis, and in vitro transcription was carried out using an Agilent Low RNA input fluorescent linear amplification kit (Agilent Technologies). The fluorescent cRNA was used for oligomicroarray hybridization at the Biomedicum Biochip Center (Helsinki, Finland). The hybridization solution was prepared by using an in situ hybridization kit plus reagents (Agilent Technologies). Four technical replicates of Agilent microarrays were hybridized overnight at +60°C. The replicates included two dye-swap analyses for both PC-3/mock and PC-3/FGF-8b samples, swapping the dyes used for each of the RNA samples. After hybridization, the slides were scanned and analyzed using an Agilent microarray scanner system and Feature Extraction software, as recommended by the manufacturer. Spots that did not pass quality control procedures in the Feature Extraction software were flagged and removed from further analysis. Raw microarray data was deposited with the public repository Array Express (www.ebi.ac.uk/arrayexpress).

Agilent Mouse two-color cDNA microarrays containing 9,607 features were used for studying gene expression differences between PC-3/mock and PC-3/FGF-8b mouse orthotopic prostate tumors at the 8-week time point, as shown in Figure 6b. Total RNA of separate tumors was used for cDNA synthesis, and in vitro transcription was carried out using an Agilent Direct labeling kit (Agilent Technologies) in the presence of Cy3– and Cy5–dCTP. Two biological replicates of PC-3/FGF-8b tumors and three biological replicates of PC-3/mock tumors were hybridized to chips separately. Both PC-3/FGF-8b samples were hybridized with each PC-3/mock sample so that there were six hybridizations altogether. Hybridization and data acquisition were carried out in a similar fashion as for the Agilent Human oligomicroarrays in this study.

MICROARRAY DATA ANALYSIS

Gene Spring 7.2 software (Agilent Technologies) was used for analysis of the first array data (Fig. 6a, PC-3/mock vs. PC-3/FGF-8b cell human microarray data). Agilent Feature Extraction software applies Lowess normalization to the data. Per spot and per chip normalization procedures were further applied to the data. To be included in the analysis, a gene had to have a *t*-test *P*-value of <0.05 in all inspected conditions. A criterion of a more than twofold difference between test (PC-3/FGF-8b) and control (PC-3/mock) expression values was further set. After normalization a total of 19,925 genes passed the quality filtering, 43 genes were found to be significantly deviated and more than twofold upregulated and 126 genes were downregulated when comparing PC-3/FGF-8b versus PC-3/mock cells (Supplementary Table SI). For annotation and analysis of the function of these up- and downregulated genes, PubMed and GeneSpring tools were first exployed by using GenBank Accession numbers, UniGene Cluster Numbers, Locus Link gene symbols (NCBI, NIH), and GO (Gene Ontology) terms. Ingenuity Pathways Analysis (IPA, Ingenuity Systems, http://www.ingenuity.com) was also used for mining analysis of the microarray data. This system uses a database (Ingenuity Pathways Knowledge Base) that constructs functional regulatory networks from a list of genes. Significantly up- or downregulated (focus) genes were used as starting points for generating networks. For network building, the program uses focus genes and its database to identify network interactions. A statistical score of a negative log of *P* was determined, denoting the likelihood of the focus genes in the network being found together as a result of chance. Fisher's exact test was used to calculate *P*-values. We then did additional analysis with IPA for a wider set of focus genes having a significant *t*-test value without the twofold restriction in expression value. This analysis provided similar network results compared with the analysis described above with the more narrow set of genes (data not shown).

R software (http://www.r-project.org) was used for analysis of the mouse array data (Fig. 6b, PC-3/FGF-8b vs. PC-3/mock mouse tumor data). The data exported from Agilent Feature Extraction software were imported to R and basic quality control of the data was performed. The data were normalized by means of shift-log normalization [Kerr et al., 2002]. One-sample *t*-tests were used to detect the genes whose expression log-ratios significantly deviated from zero ($P < 0.05$). Altogether, 55 genes were found to be more than twofold upregulated and six genes were found to be more than twofold downregulated when comparing PC-3/FGF-8b versus PC-3/mock tumor samples (Supplementary Table SIV). Ingenuity Pathways Analysis and the Database for Annotation, Visualization and Integrated Discovery (DAVID, http://niaid.abcc.ncifcrf.gov/home.jsp) [Dennis et al., 2003] were used for mining analyses of the data from Agilent mouse microarrays.

RT-qPCR OF THE DIFFERENTIALLY REGULATED GENES OF CELL CLONES AND TUMORS

For RT-qPCR analysis, 2 μg of total RNA from PC-3/FGF-8b and PC-3/mock cell clones and orthotopic tumors was used for the reverse transcription to make cDNA via reverse transcriptase (M-MLV, Promega Corp., Madison, WI). Complementary DNA was amplified by DyNAzyme II DNA Polymerase (Finnzymes, Finland) with an Eppendorf Mastercycler Gradient (Eppendorf AG, Hamburg, Germany) and then diluted to 100 μl. Two microliters of the diluted cDNA was used in a probe-based RT-qPCR method called ProbeLibrary (ProbeLibrary, Roche Diagnostics GmbH, Roche Applied Science, Switzerland) in a 10 μl reaction volume. Online assay design software (ProbeFinder; http://www.universalprobelibrary.com) was used to identify suitable human and mouse primer pairs and the matching probes (for primer and ProbeLibrary probe information, see Supplementary Table SVII). Primers were made by Oligomer (Helsinki, Finland) and the human and mouse Universal Probelibrary sets were from Roche Applied Science. ProbeLibrary RT-qPCR was performed with an ABI PRISM 7700 sequence detector (Applied Biosystems) using ABgene PCR ROX master mix (ABgene, Epsom, UK) at the Turku Centre for Biotechnology (Turku, Finland). Cycling conditions were 95°C for 15 min, then 40 cycles of 15 s at 95°C and 1 min (1.5 min for GPR-4) at +60°C. Levels of the housekeeping protein glyceraldehyde-3-phosphate dehydrogenase (GAPDH) were used to normalize the data.

STATISTICAL ANALYSIS

Except for the microarray data, statistical analyses were carried out using Statistica 6.0 software (1997). The normality of distribution was tested by means of the Shapiro–Wilks *W*-test, and statistical significances of differences were tested by means of independent *t*-tests. If the groups were not normally distributed, the Mann–Whitney *U*-test was applied. Results were considered statistically significant at $P < 0.05$.

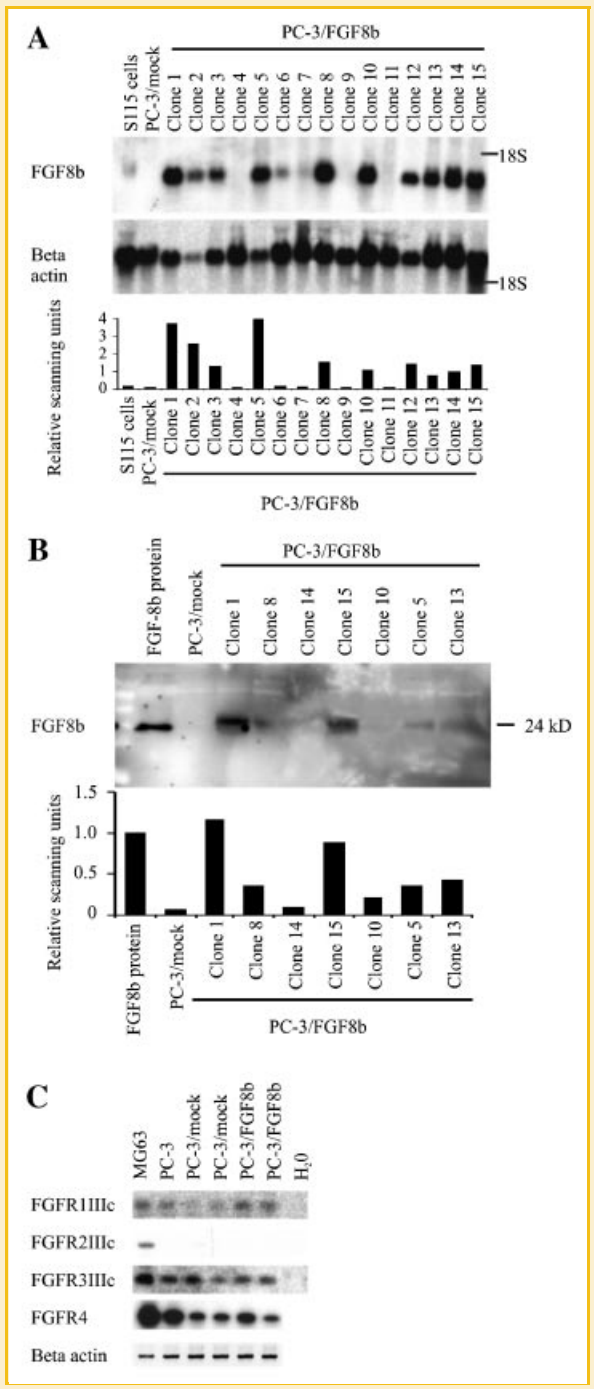

RESULTS

EXPRESSION OF ECTOPIC FGF-8b AND FGF RECEPTORS IN TRANSFECTED PC-3 CELLS

Transfected PC-3 cell clones (PC-3/FGF-8b) with high FGF-8b expression were selected for FGF-8b protein analysis (Fig. 1A,B). Clones expressing FGF-8b mRNA and protein at a very high (clone 1) and at a moderate (clone 15) level were chosen for further studies. The clones presented basically similar in vitro growth characteristics and both clones produced tumors in nude mice, although the growth rate of clone 1 in vivo was faster than that of clone 15 (data not shown). Therefore, clone 1 was selected for further experiments. PC-3 clones transfected with empty vector (PC-3/mock) and parental PC-3 cells did not express FGF-8 at a detectable level.

FGF-8b is known to signal through the FGF receptor splice forms FGFR1IIIc, FGFR2IIIc, FGFR3IIIc, and FGFR4 [MacArthur et al., 1995; Ornitz et al., 1996; Olsen et al., 2006]. In tumors FGF-8 is considered to influence tumor growth by both autocrine and paracrine mechanisms [Presta et al., 2005]. We studied the expression of mRNAs for FGF-8b receptors in PC-3 cells and in FGF-8b- and mock-transfected PC-3 cell clones by means of RT-PCR. The cells expressed the isoforms FGFR1IIIc, FGFR3IIIc, and FGFR4, but not FGFR2IIIc (Fig. 1C). FGFR2 protein was not detected in Western blotting of PC-3 parental or transfected cells with an anti-FGFR2 antibody, either (data not shown).

EFFECT OF FGF-8b ON PC-3 CELL PROLIFERATION AND MORPHOLOGY

Transfection with FGF-8b increased the proliferation of the cells approximately 1.5-fold when compared with PC-3/mock cells (Fig. 2A). The morphology of the FGF-8b-transfected cells looked more spindle-like than that of the mock-transfected (Fig. 2B) or PC-3 parental cells (data not shown). The proportion of elongated cells with protrusions was increased in cultures of FGF-8b-overexpressing

Fig. 1. Expression of mRNA and protein for FGF-8b and FGF-8b receptors in PC-3 cells and transfected PC-3 cell clones. The expression vector pcDNA3.1 containing human FGF-8 isoform b cDNA and an empty pcDNA3.1 vector (mock) were used. Plasmids were transfected into PC-3 cells using Lipofectamine™ and clones were selected in medium containing G418. Isolated colonies were cloned and characterized after expansion of the clones. A: Total RNA extracted from the cell clones was blotted on nylon membranes and hybridized with a specific probe for FGF-8b. S115 cells were used as a positive control and compared with PC-3/mock clone 1 and with PC-3/FGF-8b clones. B: The protein samples from selected cell clones were transferred to nitrocellulose membrane and immunoblotted with an anti-FGF-8b antibody. The samples were visualized using ECL detection kits. FGF-8b recombinant protein was used as a positive control and compared with PC-3/mock clone 1 and PC-3/FGF-8b clones. Corrected scanning units of FGF-8b protein expression in the different clones were quantified by using a MicroComputer Imaging Device™ (Imaging Research, Inc., Ontario, Canada). C: Total RNA from parental and transfected PC-3 cells was examined by RT-PCR. Products of FGFR1IIIc (673 bp) and FGFR3IIIc (116 bp) were confirmed with specific oligonucleotide probes and products of FGFR2IIIc (752 bp) and FGFR4 (637 bp) were confirmed by hybridization with specific cDNAs. Products were from positive controls (lane 1, MG63 cells), PC-3 parental cells (lane 2), PC-3/mock clone 1 and 2 cells (lanes 3 and 4), PC-3/FGF-8b clone 1 and 15 cells (lanes 5 and 6), and a negative control (lane 7, H_2O).

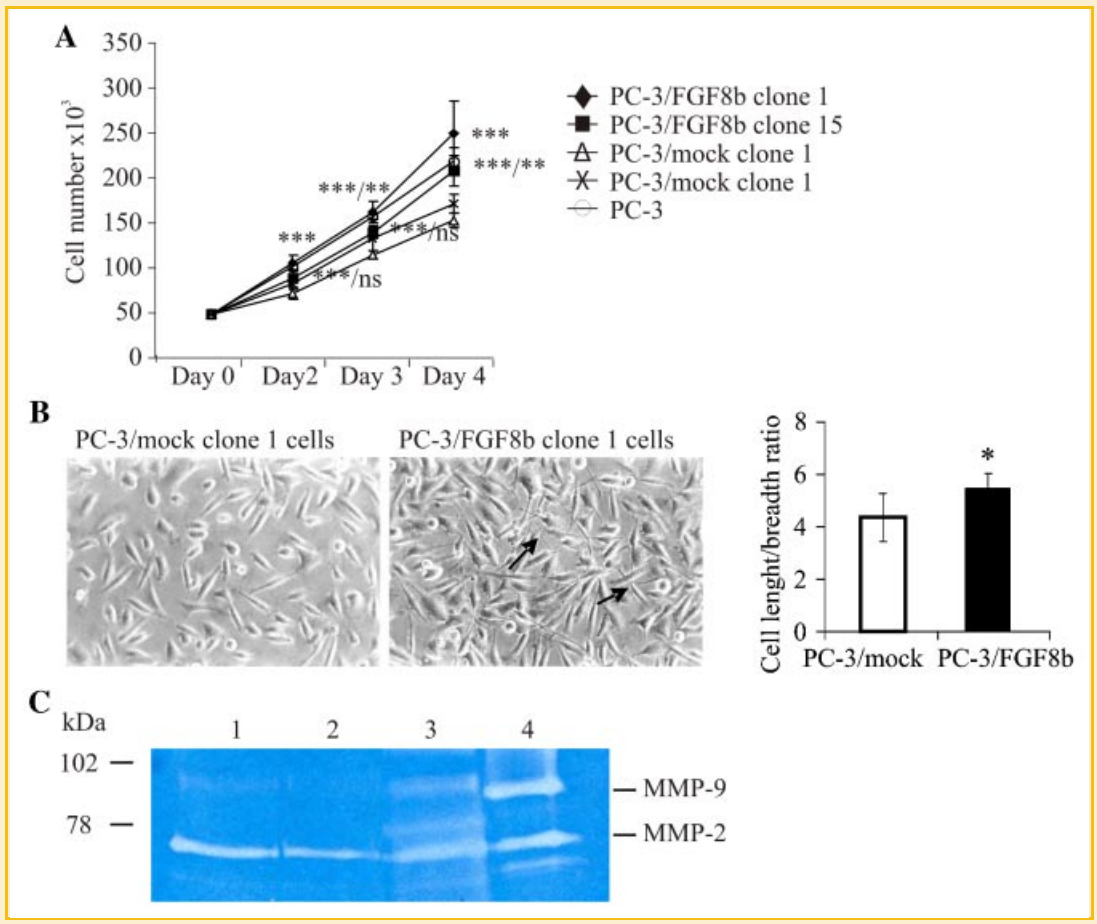

Fig. 2. In vitro characteristics of FGF-8b-transfected PC-3 cells. A: The effect of transfection of FGF-8b on the proliferation of PC-3 cells. Normality of distribution was tested by means of the Shapiro–Wilks *W*-test, and an independent *t*-test was used to test the statistical significance of differences between the PC-3/FGF-8b and PC-3/mock clones. Asterisks indicate statistically significant differences between PC-3/FGF-8b and PC-3/mock clones; ns, not significant; $^{**}P < 0.01$; $^{***}P < 0.001$. Where two *P*-values are shown for a designated PC-3/FGF-8b clone time point, the first one shows comparison with the PC-3/mock 1 and the second one comparison with the PC-3/mock 2 clone. Where only one *P*-value is shown for a designated PC-3/FGF-8b clone time point, the value shows comparison with both PC-3/mock clones. The study was carried out twice and similar results were obtained. B: The morphology of FGF-8b-transfected PC-3 cells in culture. Arrows point to cells that were considered elongated. Bar, 50 μm. Cell length/breadth ratio of PC-3 cells was calculated, the normality of distribution was tested by means of Shapiro–Wilks *W*-test, and independent *t*-test was used to test the statistical significance of difference between PC-3/FGF-8b and PC-3/mock. C: Serum-free DMEM was conditioned by parental or transfected clones of PC-3 cells and lyophilized. Samples were then subjected to electrophoresis in 10% SDS–PAGE containing gelatin. Gelatinolytic activities of MMP-9 and MMP-2 are observed as transparent bands in Coomassie Blue-stained gel. Lane 1, PC-3 cells, lane 2, PC-3/mock cells, lane 3, PC-3/FGF-8b cells, lane 4, conditioned medium from HT-1080 human fibrosarcoma cells was used as a positive control for MMP-9 and MMP-2. The assay was repeated three times and similar results were obtained. [Color figure can be viewed in the online issue, which is available at www.interscience.wiley.com.]

cells (Fig. 2B, $P < 0.05$). We also investigated whether FGF-8b affects MMP production in vitro, since previous studies have shown that FGFs increase MMP expression in prostate cancer cells [Udayakumar et al., 2004]. Figure 2C shows the gelatinolytic activity corresponding to MMP-9 was increased in the medium of FGF-8b expressing cells compared with mock-transfected or parental cells. We did not find any changes between the cells in the activity of MMP-2. The experiment was repeated three times and similar results were gained.

PRODUCTION OF FGF-8b-EXPRESSING PC-3 TUMORS

PC-3/FGF-8b and PC-3/mock cells were inoculated subcutaneously and orthotopically into nude mice to study the effects of FGF-8b on prostate tumor growth in vivo. The subcutaneous tumors were grown for 6 weeks. The mice with orthotopic tumors were sacrificed 4 or 8 weeks after inoculation. A high level of FGF-8b expression in sc and orthotopic PC-3/FGF-8b prostate tumors compared with PC-3/mock tumors was confirmed by Northern blotting (Fig. 3A). The RT-PCR technique was used to study the expression of receptors for FGF-8b. Although the transfected PC-3 cells did not show expression of FGFR2IIIc in vitro, the tumors expressed the FGFR2IIIc isoform (Fig. 3B). As regards other receptor isoforms, the expression pattern remained basically unaltered. FGFR2IIIc is usually expressed in cells of mesenchymal origin in the prostate [Yan et al., 1993]. Considering the lack of FGFR2 mRNA and protein expression in PC-3 parent and transfected cells it is probable that the signal in RT-PCR of tumor tissue was derived from surrounding normal prostate stroma infiltrated by tumor tissue.

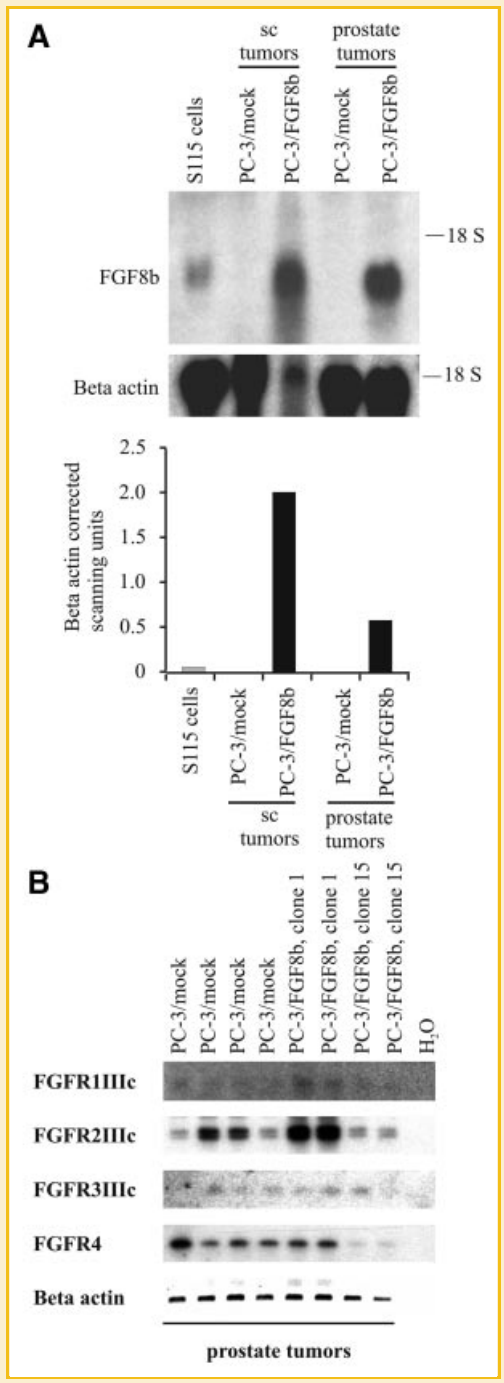

Fig. 3. Expression of mRNA for FGF-8b and FGF-8b receptors in tumors formed by PC-3/FGF-8b cells. A: Expression of mRNA for FGF-8b in subcutaneous (sc) tumors at 4 weeks after cancer cell inoculation and in orthotopic prostate tumors 8 weeks after cancer cell inoculation into the prostates of nude mice. Total RNA extracted from the tumors was blotted on nylon membranes and hybridized with a specific probe for FGF-8b. B: Total RNA from transfected orthotopic PC-3 tumors was examined by RT-PCR. Products of FGFR1IIIc (673 bp) and FGFR3IIIc (116 bp) were confirmed with specific oligonucleotide probes and products of FGFR2IIIc (752 bp) and FGFR4 (637 bp) were confirmed by hybridization with specific cDNAs. Products were from PC-3/mock tumors (lanes 1–4), PC-3/FGF-8b clone 1 tumors (lanes 5–6), PC-3/FGF-8b clone 15 tumors (lanes 7–8) and a negative control (lane 9, H_2O). Positive controls for each FGFR can be seen in Figure 1C.

EFFECT OF FGF-8b ON PC-3 TUMOR GROWTH AND METASTASIS

Subcutaneous PC-3/FGF-8b tumors ($n = 30$) were statistically significantly larger than PC-3/mock sc tumors ($n = 22$) as early as 3 weeks after inoculation of cancer cells ($P < 0.001$) and the difference continued to increase throughout the 6-week study period (Fig. 4A). Next, PC-3/FGF-8b and PC-3/mock cells were grown as orthotopic tumors in the prostates of nude mice. PC-3/FGF-8b tumors ($n = 4$) were slightly bigger than PC-3/mock tumors ($n = 6$) at 4 weeks after cancer cell inoculation, but this result was not statistically significant (Fig. 4A, $P = 0.082$). At 8 weeks after inoculation of cancer cells, PC-3/FGF-8b ($n = 6$) tumors were clearly larger than PC-3/mock tumors ($n = 9$, $P < 0.01$, Fig. 4A). PC-3/FGF-8b clone 15 tumors were also significantly larger ($n = 5$, 220.4 $mm^3 \pm 79.3$ mm^3) than PC-3/mock tumors ($n = 4$, 70.2 $mm^3 \pm 44.7$ mm^3, $P < 0.05$) at 4 weeks after inoculation of cancer cells (data not shown).

PC-3 tumors are known to metastasize to prostate-draining iliac and sacral lymph nodes [Tuomela et al., 2008]. At 8 weeks, metastases were found in regional lymph nodes in 100% of PC-3/FGF-8b tumor bearing mice ($n = 6/6$) and in 78% of PC-3/mock tumors bearing mice ($n = 7/9$), but this difference was not statistically significant ($P = 0.21$). The relative area of metastasis/lymph node was analyzed in tissue sections taken from several levels ($n = 8$–14) of the tissue but no statistically significant differences were found between PC-3/FGF-8b- and PC-3/mock cell-inoculated animals (data not shown). Lung metastases were found in two mice bearing PC-3/FGF-8b tumors, sacrificed 8 weeks after inoculation, but none in the PC-3/mock groups. No metastases were found in other organs by histological examination. However, when using RT-qPCR we found an increased amount of FGF-8b mRNA in the lungs of mice that had been orthotopically inoculated with PC-3/FGF-8b cells compared with PC-3/mock mice (Fig. 4B, $P < 0.05$). Interestingly, a similar trend was seen in serum, liver and bone marrow of mice that had been orthotopically inoculated with PC-3/FGF-8b cells compared with PC-3/mock cells, but these differences did not reach statistical significance (data not shown).

EFFECT OF FGF-8b ON PC-3 TUMOR MORPHOLOGY

Macroscopic and microscopic analysis revealed strikingly increased vessel-like formation in PC-3/FGF-8b orthotopic tumors compared with PC-3/mock tumors (Fig. 5A–H). These capillary-like structures were wide and distorted. Histomorphometric analysis revealed that PC-3/FGF-8b tumors contained significantly more capillary-like structures than PC-3/mock tumors (Fig. 5I, $P < 0.01$, orthotopic and $P < 0.001$, subcutaneous). The endothelial-specific CD31 staining of the subcutaneous tumors was clearly increased in the FGF-8b-transfected tumors (Fig. 5J, $P < 0.001$). In addition, endothelial cell-specific CD34 immunohistochemical staining of the tumors was increased in orthotopic and subcutaneous PC-3/FGF-8b tumors compared with PC-3/mock tumors, although the difference did not reach statistical significance (data not shown). The proliferation rate of the orthotopic tumors was determined using Ki67 immunostaining, which showed an increased number of proliferating cells in PC-3/FGF-8b orthotopic tumors compared with PC-3/mock tumors (Fig. 5K, $P < 0.05$).

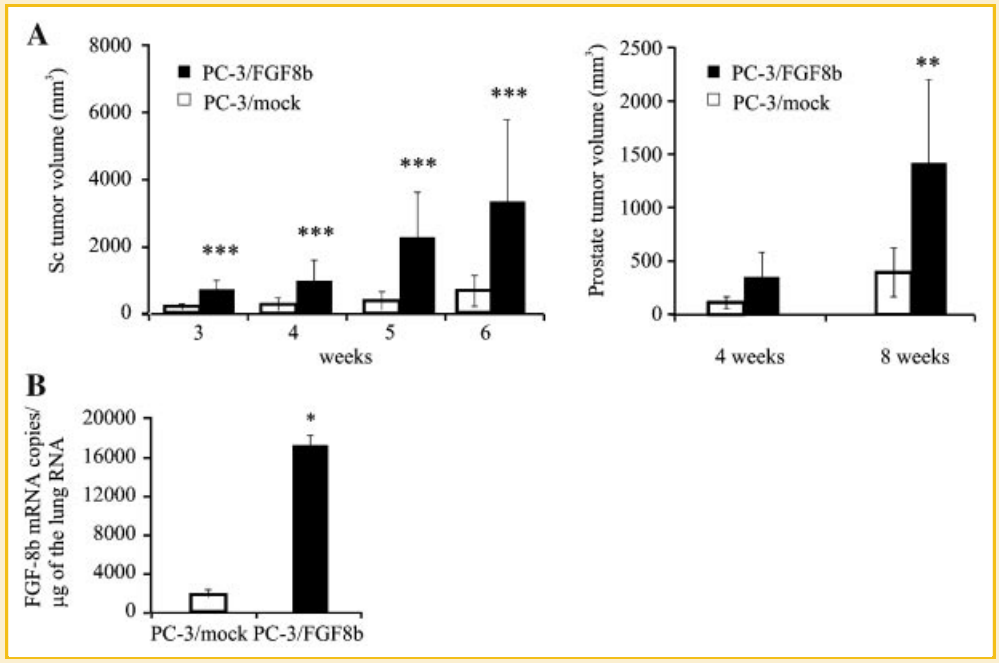

Fig. 4. Effect of ectopic FGF-8b on growth and metastasis of PC-3 tumors. A: The effect of transfection of FGF-8b or an empty mock vector into PC-3 cells on sc tumor growth 3–6 weeks after inoculation of cancer cells into nude mice and the effect of FGF-8b transfection on orthotopic PC-3 tumor growth 4 and 8 weeks after inoculation of cancer cells into the prostates of nude mice. Normality of distribution was tested by means of the Shapiro–Wilks *W*-test, and an independent *t*-test was used to test the statistical significance of differences between the sizes of PC-3/FGF-8b and PC-3/mock tumors. Asterisks indicate statistically significant differences between PC-3/FGF-8b and PC-3/mock tumors; $^{**}P < 0.01$; $^{***}P < 0.001$. B: RT-qPCR analysis of lung samples showed increased copy numbers of FGF-8b mRNA in lungs of PC-3/FGF-8b mice compared with those of PC-3/mock mice; $^{*}P < 0.05$.

DNA MICROARRAY ANALYSIS OF FGF-8b RESPONSIVE GENES IN PC-3 CELLS AND TUMORS

We used DNA microarrays to study the possible mechanisms behind FGF-8b-induced growth, angiogenic-like morphology and spread of the tumors. Two microarray analyses were performed, as shown in Figure 6.

Human oligoarrays were used to compare mRNA from PC-3/FGF-8b and PC-3/mock cells (Fig. 6A). This analysis revealed 43 more than twofold upregulated and 126 more than twofold downregulated genes (Table II and Supplementary Table SI). GeneSpring Gene Ontology (GO) tools were used to analyze these differentially expressed genes in PC-3 cells. In this analysis the number of genes expected to occur randomly in each GO group is compared with the actual distribution of differentially expressed genes. On the basis on this, a list of biological functions that are statistically overexpressed is created. The predominantly overrepresented GO groups associated with FGF-8-induced genes in PC-3 cells were those pertaining to cell communication, response to external stimulus and development (Supplementary Table SIIA). The statistically most enriched GO category for genes downregulated by FGF-8b in PC-3 cells was energy metabolism (Supplementary Table SIIB), which was associated with coenzymes and prosthetic group metabolism, energy pathways and electron transport.

Ingenuity Pathway Analysis (IPA) was used as an additional tool for investigating the biological pathways that the differentially expressed genes represent. In IPA, genes are distributed into networks defined by published interactions and then these networks are associated with defined with biological pathways. The analysis involves different statistical methods and a different database compared with GO analysis (see Materials and Methods Section). Using IPA we identified two statistically significant networks associated with several FGF-8-induced genes in PC-3 cells (Supplementary Table SIIIA). These IPA-generated networks were associated with embryonic development, cellular growth and proliferation, cellular movement, gene expression, DNA replication, recombination and repair. We then identified six statistically significant networks associated with several of the FGF-8-repressed genes (Supplementary Table SIIIB), three of which were associated with cell death. One network was associated with energy production, nucleic acid metabolism, and small molecule biochemistry.

The mouse microarray analysis was performed in order to study primarily the effects of FGF-8b on host-derived stromal components of orthotopic PC-3 prostate tumors (Fig. 6B). Agilent's Mouse two-color cDNA microarrays were used to study differences between the expression of PC-3/FGF-8b and PC/mock tumors grown for 8 weeks. All tumors were studied separately. These analyses revealed 55 over twofold upregulated and 6 over twofold downregulated genes (Table III and Supplementary Table SIV). As in the microarray analysis of FGF-8b versus mock cells, development and response to external stimulus were among the statistically overrepresented GO biological function categories in the FGF-8-induced genes in tumors (see Supplementary Tables SV and SIIA). Using IPA we found an association between several upregulated genes (Supplementary Table SVI), related to cell-to-cell signaling and interaction and

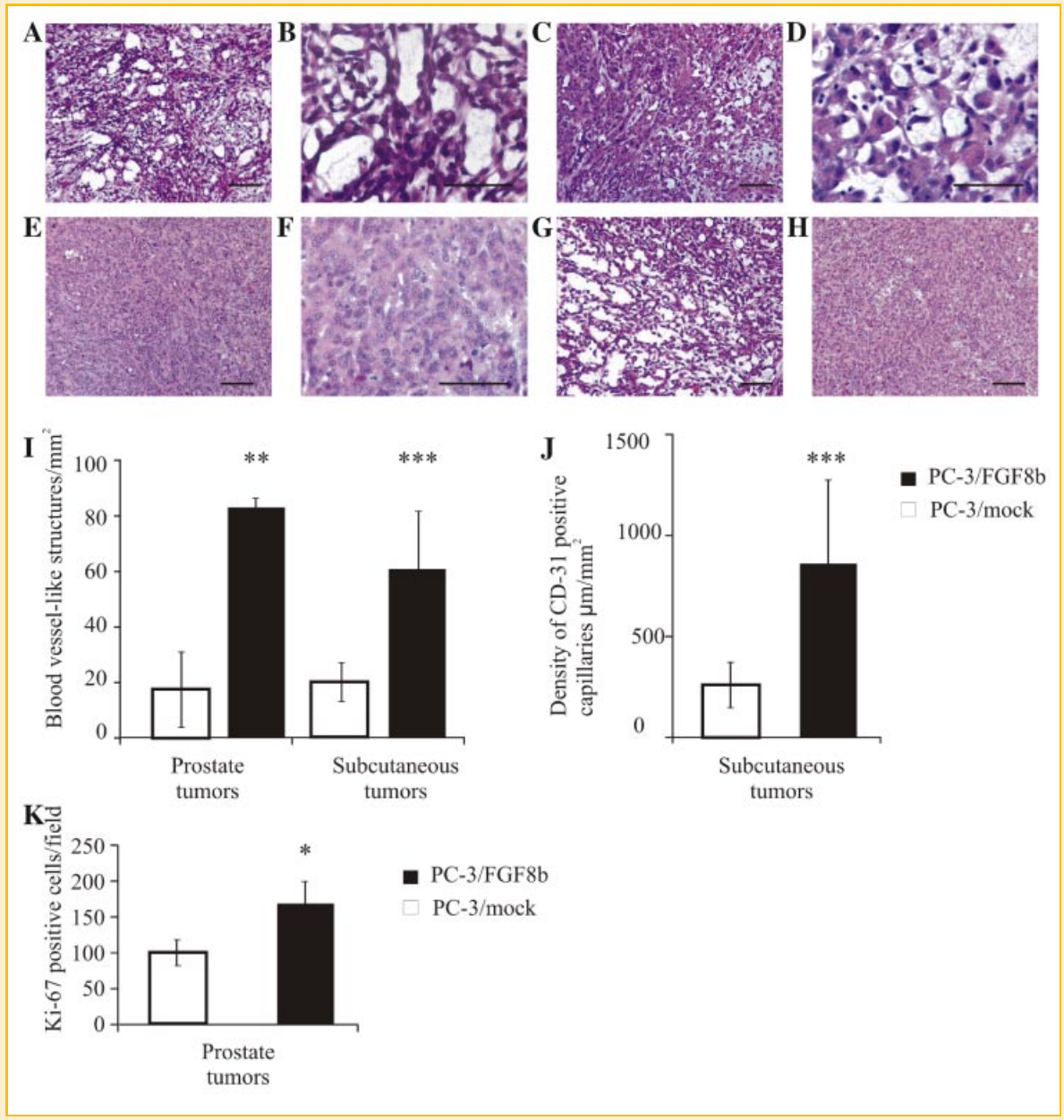

Fig. 5. Effect of ectopic expression of FGF-8b on morphology of orthotopic and subcutaneous PC-3 tumors. H&E staining of PC-3/FGF-8b clone 1 (A,B), PC-3/FGF-8b clone 15 (C,D) and PC-3/mock prostate tumors (E,F), and PC-3/FGF-8b clone 1 (G) and PC-3/mock sc tumors (H). Bar, 100 μm. I: Number of vessel-like formations/mm^2 of tumor area was counted in multiple sections. J: Density of CD31-positive vessels/mm^2 of tumor area was counted. K: Numbers of Ki67-positive cells/field of view in multiple views of tumor area were counted. Normality of distribution was tested by means of the Shapiro–Wilks *W*-test, and an independent *t*-test was used to test the statistical significance of differences between the different parameters of PC-3/FGF-8b and PC-3/mock tumors. Asterisks indicate statistically significant differences between PC-3/FGF-8b and PC-3/mock tumors; $^{*}P < 0.05$; $^{**}P < 0.01$, $^{***}P < 0.001$. [Color figure can be viewed in the online issue, which is available at www.interscience.wiley.com.]

cellular growth and proliferation. Other IPA categories among the FGF-8-induced genes in the prostate tumors included post-translational modification, cell death, organism injury and abnormalities, hematological system development and function, inflammatory disease and tissue morphology. No statistically significant GO groups or IPA networks were found as regards downregulated genes in the array of tumor samples.

RT-qPCR CONFIRMATION OF DIFFERENTIAL EXPRESSION OF SELECTED GENES IN PC-3/FGF-8b CELL LINES AND TUMORS

RT-qPCR analysis of RNA from PC-3/FGF-8b and PC-3/mock cell clones and the orthotopic PC-3/FGF-8b and PC-3/mock tumors was carried out to confirm the microarray results (Fig. 7 and Supplementary Fig. S1A). First, 11 genes obtained from the microarray of PC-3 cells (*ATP5G3*, *CRIP1*, *DDAH2*, *FGF-8b*,

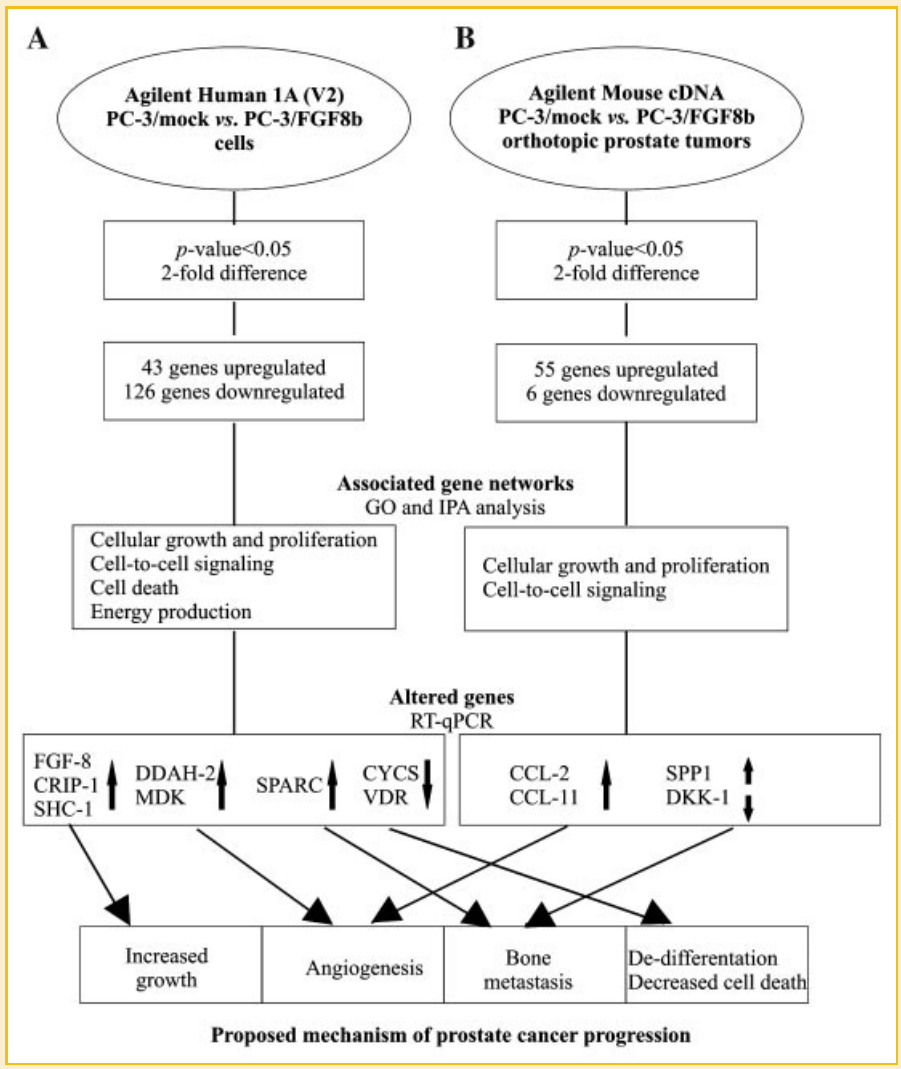

Fig. 6. Data flow and summary of results of microarray analysis. Arrays were set up for PC-3/FGF-8b and PC-3/mock cells on Agilent Human 1A (V2) oligo microarrays (A) and for mouse orthotopic PC-3/FGF-8b and PC-3/mock prostate tumors on Agilent Mouse two-color cDNA microarrays (B). The numbers of statistically significantly altered genes (*P*-value of <0.05, more than twofold difference between expression values) are shown. Gene Ontology (GO) terms and Ingenuity Pathways Analysis (IPA) were used to analyze the data. Data were verified by RT-qPCR. For more detailed information, see Materials and Methods Section. A summary is shown of transcriptional changes caused by FGF-8b, which could result in prostate cancer progression in mouse bearing orthotopic PC-3 prostate tumors. Arrows pointing up indicate upregulated genes. Arrows pointing down indicate downregulated genes.

GPR4, *LOC126755*, *MIG-6*, *SHC1*, *SLC22A17*, *SPARC*, and *VDR*) were studied. In most cases, the pattern of transcript abundance of those genes was consistent with the microarray data from PC-3 cells (Fig. 7 and Supplementary Fig. S1A). Changes in FGF-8b-induced gene expression in cell lines could also be recapitulated in most of the eight tumor samples studied (Fig. 7, Supplementary Fig. S1A). Then, FGF-8b-induced changes of gene expression of mouse orthotopic PC-3 prostate tumors observed in microarrays were verified by RT-qPCR of selected eight genes (*DKK-1*, *ENOS*, *AKR1B8*, *GTSM1*, *NEF1*, *SPP1*, *PPP1CB*, and *VEGF-B*) using mouse-specific primers. These results were reproducible in most of the six tumor samples analyzed (Fig. 7 and Supplementary Fig. S1B). We performed an additional sequence analysis of the used mouse primers to verify that they where highly mouse-specific, which should minimize detection of tumor cell derived human cDNAs from tumor.

DISCUSSION

Advanced and metastatic prostate cancer is often castration resistant and associated with a high degree of morbidity and few treatment options. Investigation of the molecular mechanisms of prostate cancer growth is needed to identify aggressive cancers. FGF-8 is overexpressed in a marked proportion of aggressive prostate cancers [Tanaka et al., 1998; Valve et al., 2001; Gnanapragasam et al., 2003] but its molecular targets and involvement in malignant growth

TABLE II. Human Microarray Analysis Results Concerning Differentially Expressed Genes in FGF-8-Transfected PC-3 Cells In Vitro on Human Arrays: (A) Upregulated Genes, (B) Downregulated Genes

(A)	Accession no.	Common name	Description	Fold increase
1	NM_006119	FGF-8	Fibroblast growth factor 8, transcript variant B	16.91
2	NM_001311	CRIP1	Cysteine-rich protein 1 (intestinal)	4.44
3	NM_133467	CITED4	Cbp/p300-interacting transactivator	3.41
4	U09770	hCRHP	Human cysteine-rich heart protein	3.24
5	NM_019105	TNXB	Tenascin XB transcript variant XB	3.17
6	NM_198587	RGS12	Regulator of G-protein signaling 12, transcript variant 7	3.05
7	A_23_P66347	A_23_P66347	Unknown	2.94
8	NM_003302	TRIP6	Thyroid hormone receptor interactor 6	2.94
9	NM_005282	GPR4	G protein-coupled receptor 4	2.80
10	NM_030582	COL18A1	Collagen, type XVIII, alpha 1, transcript variant 1	2.82
11	NM_013974	DDAH2	Dimethylarginine dimethylaminohydrolase 2	2.71
12	NM_144601	CKLFSF3	Chemokine-like factor super family 3, transcript variant 1	2.74
13	D87447	D87447	mRNA for KIAA0258 gene, partial cds	2.69
14	NM_003118	SPARC	Osteonectin	2.64
15	NM_024330	SLC27A3	Solute carrier family 27 (fatty acid transporter), member 3	2.56
16	NM_003273	TM7SF2	Transmembrane 7 superfamily member 2	2.58
17	NM_178502	DTX3	Deltex 3 homolog (Drosophila)	2.53
18	NM_003782	B3GALT4	UDP-Gal:betaGlcNAc beta 1,3-galactosyltransferase, polypeptide 4	2.47
19	NM_178335	C3orf6	Chromosome 3 open reading frame 6	2.44
20	NM_005361	MAGEA2	Melanoma antigen, family A, 2, transcript variant 1	2.42

(B)	Accession no.	Common name	Description	Fold decrease
1	BC016048	BC016048	Hypothetical protein LOC126755	0.06
2	AL834409	AL834409	Reticulon 4 receptor-like 1	0.11
3	NM_016609	SLC22A17	Solute carrier family 22 member 17 transcript variant 2	0.12
4	NM_012119	CCRK	Cell cycle-related kinase, transcript variant 2	0.18
5	NM_017823	NM_017823	Dual specificity phosphatase 23	0.20
6	NM_033512	TSPYL5	TSPY-like 5	0.23
7	NM_153350	NM_153350	Hypothetical protein MGC33974	0.24
8	THC1891253	THC1891253	Unknown	0.25
9	NM_012081	ELL2	Elongation factor, RNA polymerase II	0.25
10	NM_013363	PCOLCE2	Procollagen C-endopeptidase enhancer 2	0.28
11	NM_013300	NM_013300	Protein predicted by clone 23733 (HSU79274)	0.30
12	NM_000228	LAMB3	Laminin, beta 3	0.32
13	NM_018948	MIG-6	Mitogen-inducible gene 6	0.33
14	NM_001885	CRYAB	Crystallin, alpha B	0.34
15	A_23_P258114	A_23_P258114	Unknown	0.34
16	NM_031426	C9orf58	Chromosome 9 open reading frame 58	0.34
17	NM_173549	NM_173549	Hypothetical protein FLJ39553	0.34
18	NM_139207	NAP1L1	Nucleosome assembly protein 1-like 1, transcript variant 1	0.34
19	NM_000987	RPL26	Ribosomal protein L26	0.35
20	NM_006713	PC-4	Activated RNA polymerase II transcription cofactor 4	0.35
21	NM_004350	RUNX3	Runt-related transcription factor 3	0.36
22	NM_145307	PLEKHK1	Pleckstrin homology domain containing, family K member 1	0.36
23	NM_003064	SLPI	Secretory leukocyte protease inhibitor (antileukoproteinase)	0.36
24	AK092499	AK092499	cDNA FLJ35180 fis	0.36
25	NM_016084	RASD1	RAS, dexamethasone-induced 1	0.36

To be included in the analysis, a gene had to have a *t*-test *P*-value of <0.05 in all inspected conditions. A criterion of a more than twofold difference between test (PC-3/FGF-8b) and control (PC-3/mock) expression values was further set. (A) Forty-three genes were found to be significantly deviated and over twofold upregulated when comparing PC-3/mock versus PC-3/FGF-8b samples. Twenty genes with the highest upregulation are shown. (B) One hundred twenty-six genes were found to be significantly deviated and over twofold downregulated when comparing PC-3/mock versus PC-3/FGF-8b samples. Twenty-five genes with the highest downregulation are shown.

mechanisms are not known. In this study, we produced experimental FGF-8b-expressing PC-3 prostate tumors grown subcutaneously or orthotopically in nude mice. The orthotopic PC-3 prostate tumor model form local tumors in a relevant stromal and vascular context and send metastases to prostate-draining lymph nodes [Tuomela et al., 2008]. Our results demonstrate that FGF-8b expression caused angiogenic tumors with a highly increased rate of tumor growth associated with some changes in tumor metastasis. Microarray analyses were used to recognize FGF-8b-regulated genes associated with these phenomena.

Ectopic expression of FGF-8 stimulated the rate of proliferation of PC-3 cells in vitro as previously shown [Song et al., 2000; Heer et al., 2004]. FGF-8 also strongly enhanced the growth of subcutaneous and orthotopic prostate tumors. In addition, the proliferative effect of FGF-8b was demonstrated by increased Ki67 staining of the orthotopic tumor sections. The strikingly increased angiogenesis in the FGF-8b-transfected tumors may also partly explain the rapid tumor growth. An increased number of CD31-positive endothelial cells, demonstrative of angiogenesis, were observed in subcutaneous tumors. FGFs, among other factors such as vascular endothelial growth factors (VEGFs), are considered to be key regulators of prostate cancer angiogenesis, which supports tumor growth [Doll et al., 2001; Huss et al., 2003]. We have previously shown that FGF-8b increases the angiogenic capacity of breast cancer cells and vessel sprouting in a chorion allantoic membrane assay [Mattila et al., 2001; Ruohola et al., 2001]. Expression of VEGF and FGF-8 and the

TABLE III. Mouse Microarray Analysis Results Concerning Differentially Expressed Genes in FGF-8-Transfected PC-3 Orthotopic Tumors In Vivo on Mouse Arrays: (A) Upregulated Genes, (B) Downregulated Genes

A	Accession no.	Common name	Description	Fold increase
1	AA563324	SPP1	Secreted phosphoprotein 1 (osteopontin)	7.58
2	AI605648	SPRR2A	Small proline-rich protein 2A	6.82
3	AA067003	GSTM1	Glutathione S-transferase, M 1	6.53
4	AA028420	SPRR1A	Small proline-rich protein 1A	4.55
5	AA207872	REN1	Renin 2 tandem duplication of Ren1	4.39
6	AA624690	AKR1B8	Aldo-keto reductase family 1, member B8	4.13

B	Accession no.	Common name	Description	Fold decrease
1	W79975	DKK-1	Dickkopf homolog 1 (*Xenopus laevis*)	0.36
2	W99951	NEFL	Neurofilament, light polypeptide	0.46
3	AA796818	EST	Interferon-stimulated protein (15 kDa)	0.46
4	AA611441	TPI1	Triosephosphate isomerase	0.46
5	AA450763	PGK1	Phosphoglycerate kinase 1	0.48
6	AA438025	PPP1CB	Protein phosphatase 1, catalytic subunit, beta isoform	0.49

(A) Fifty-five genes were found to be significantly deviated and over twofold upregulated when comparing PC-3/mock versus PC-3/FGF-8b tumor samples on mouse arrays. Six genes with the highest upregulation are shown. (B) Six genes were found to be significantly deviated and over twofold downregulated when comparing PC-3/mock versus PC-3/FGF-8b tumor samples. When comparing these results with human array analysis between PC-3/FGF-8b and PC-3/mock cells (Table II), it should be kept in mind that different arrays, normalization protocols and analysis programs were used.

clinico-pathologic parameters of human prostate cancer correlate with each other [West et al., 2001]. In our FGF-8 expressing tumors most vascular-like structures in the tumors were, however, wide and tortuous and they did not stain for CD34, another endothelial marker. It is possible that these capillary-like structures are not fully matured capillaries. FGFs may thus not be able to induce mature capillaries alone. Accordingly, it has been previously shown that a synergistic effect between platelet-derived growth factor (PDGF) and FGF-2 is required to produce mature and fully functional capillaries in neoangiogenesis [Cao et al., 2003]. The viability and fast growth rate of the tumors in our study imply, however, that these capillaries were able to support tumor growth relatively efficiently.

Our results also showed that ectopic overexpression of FGF-8b increased MMP-9 production in the PC-3 cells. This finding is in line with our previous results showing that FGF-8 induces MMP-9 production in breast cancer cells [Ruohola et al., 2001] and other studies, showing that FGF-8 increases prostate cancer cell invasion [Song et al., 2000]. In addition, the observed induction of MMP-9 may play a role in prostate cancer associated vessel formation as well as PC-3 tumor angiogenesis [Pepper, 2001; London et al., 2003]. It remains unknown if FGF-8b regulates MMP-9 production directly and what other factors are required to facilitate invasion.

The dense vascular network in orthotopic PC-3/FGF-8b prostate tumors may be associated with an increase in lung metastasis as observed by means of RT-qPCR of FGF-8b mRNA expression in serum and lungs. FGF-8b did not seem to affect invasion of tumor cells to regional lymph nodes, which represents the primary metastatic site via lymphatic pathways, but it may have facilitated hematogenous metastasis to distant organs such as the lung. It is obvious, however, that FGF-8b contribution to hematogenous metastasis may need synergistic action of other angiogenic factors (such as other FGFs, VEGFs, and PDGF). In addition, our previous results [Valta et al., 2006, 2008] show that once FGF-8b-expressing prostate cancer cells reach bone marrow, FGF-8b strongly enhances and modulates the formation of osteosclerotic bone metastases.

Gene network (IPA) and Gene Ontology (GO) analyses of the microarray data showed that FGF-8-induced genes are over-represented in developmental pathways and in cell growth and proliferation and cell-to-cell signaling pathways. Overrepresentation of energy production and nucleic acid metabolism pathways was found in both analyses of FGF-8-repressed genes. Using IPA we also found cell death associated genes (e.g., hara-kiri, *HRK*; ribosomal protein S3A, *RPS3A*; and cytochrome *c*, *CYCS*) among FGF-8b-downregulated genes. In line with the angiogenic-like morphology of the FGF-8b-expressing tumors, microarray analyses and RT-qPCR of FGF-8b-expressing PC-3 cells revealed induction of several transcripts with tumor growth and angiogenic potential (see Figs. 6 and 7), such as dimethylarginine dimethylaminohydrolase 2; *DDAH2* [Kostourou et al., 2002, 2003; Pucci-Minafra et al., 2008], midkine; *MDK* [Stoica et al., 2002], *SPARC* [Jendraschak and Sage, 1996], Src homology 2 domain containing transforming protein 1; *SHC1* [Saucier et al., 2004] and cystatin-related protein-1; *CRIP1* [Dube et al., 1998].

Vitamin D has anti-tumor effects on prostate cancer [Krishnan et al., 2003] and a recent study revealed that vitamin D3 suppresses the transcription of FGF-8 in breast cancer cells [Kawata et al., 2006]. We found that vitamin D receptor (*VDR*) and a protein associated with its activity, calbindin (*CALB1*) were significantly downregulated by FGF-8b in PC-3 cells and/or tumors in our study. The decrease of *VDR* expression, as well as the results of IPA and GO analyses suggest that de-differentiation may be one mechanism by which FGF-8b provides tumors with a growth advantage.

Using the mouse microarray analysis of orthotopic tumors we primarily aimed to evaluate the paracrine responses of host-derived stroma and the tumor microenvironment to human tumor cell derived FGF-8b. Although we cannot fully exclude the possibility that mouse microarray and following RT-qPCR analyses also recognize human tumor derived gene expression, it is probable that the transcripts from host-derived stroma largely explain the expression patterns of tumors. In analysis of orthotopic tumors we found FGF-8 regulation of interesting genes involved in

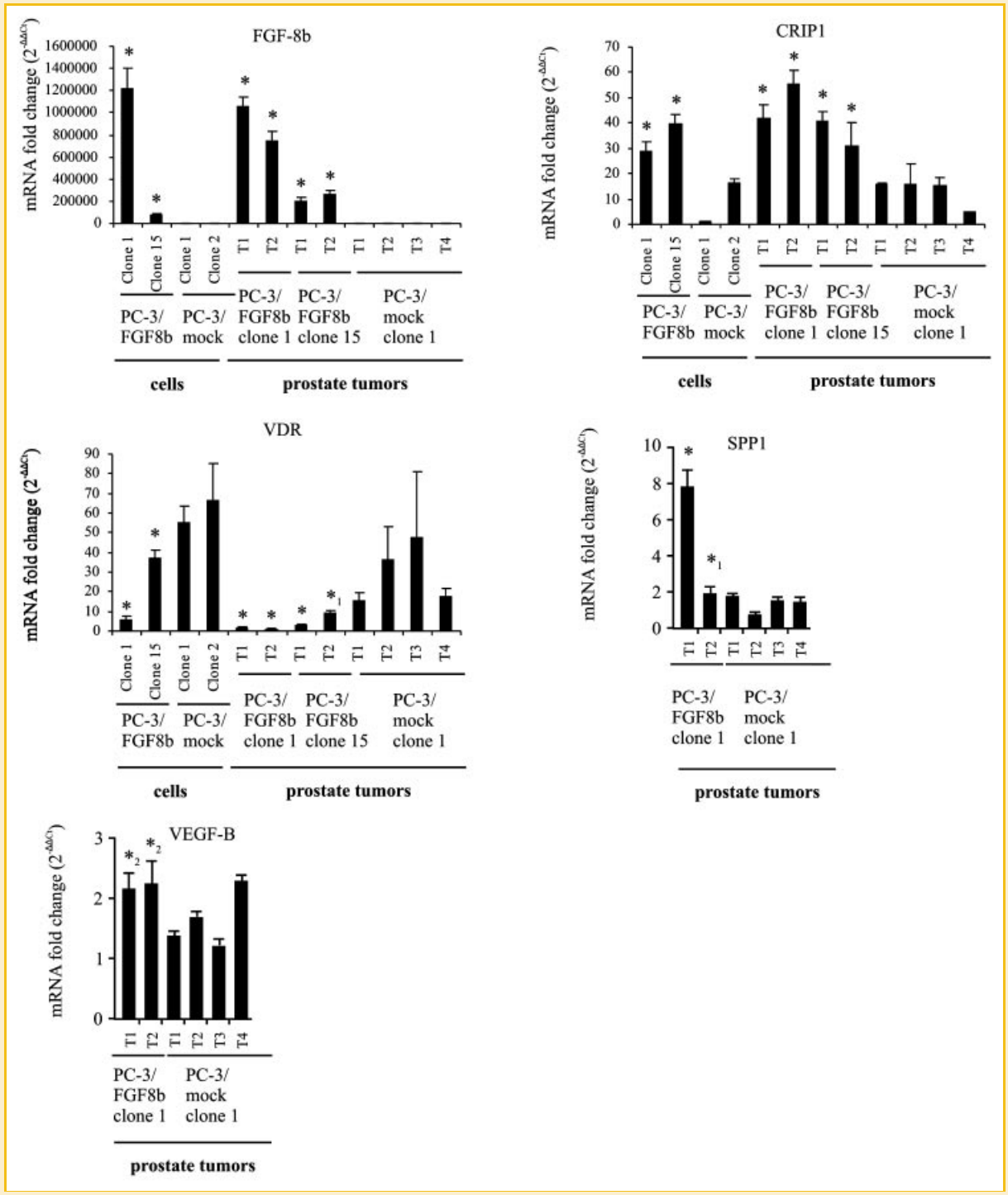

Fig. 7. RT-qPCR confirmation of the selected genes identified with microarrays. RT-qPCR was used to study the expression of various genes in PC-3/FGF-8b and PC-3/mock cell clones and orthotopic prostate tumors (T1–T4). Confirmation of PC-3 cell culture and tumor microarray data: fibroblast growth factor 8 isoform b (*FGF-8b*), cystein-rich protein-1 (*CRIP-1*), vitamin D receptor (*VDR*) osteopontin (*SPP1*) and vascular endothelial growth factor B (*VEGF-B*). The groups were not normally distributed and thus the Mann–Whitney *U*-test was applied to test the statistical significance of differences between cell clones and tumors. PC-3/FGF-8b cell clones 1 and 15 were compared with PC-3/mock clones 1 and 2. PC-3/FGF-8b clone 1 and 15 tumors were compared with PC-3/mock tumors T1–T4: $^{*}P < 0.05$; $^{*}_{1}$, $P < 0.05$ compared with PC-3/mock tumors T2–T4 only, $^{*}_{2}$, $P < 0.05$ compared with PC-3/mock tumors T1–T3 only.

angiogenesis and tumor metastasis (such as the genes for osteopontin and *DKK-1*). Angiogenic small inducible cytokine A12 (*CCL2*) [Salcedo et al., 2000] and small inducible cytokine A11/Small chemokine (C-C motif) ligand 11 (*CCL11*) [Salcedo et al., 2001] and *VEGF-B* were also upregulated in tumors.

Our finding of osteopontin (*SPP1*) induction in FGF-8b-expressing orthotopic tumors is in line with recent results, which show that *SPP1* is upregulated by FGF-8 in mouse prostate epithelium [Khodavirdi et al., 2006]. The osteopontin gene has also been shown to be upregulated by FGFR1 in prostate cancer [Freeman et al., 2003] and it has been shown to be associated with prostate cancer bone metastasis [Hotte et al., 2002]. The array of orthotopic tumors also revealed FGF-8b-associated repression of dickkopf-1 (*DKK-1*), an inhibitor of Wnts. Dickkopf-1 has been shown to block Wnt-mediated osteoblastic activity in PC-3 cells in an in vivo mouse model [Hall et al., 2005]. These findings are of special interest, keeping in mind the finding that FGF-8 is involved in prostate cancer bone metastasis [Valta et al., 2008], possibly via regulation of osteoblastic differentiation [Valta et al., 2006]. It is thus possible that FGF-8b-dependent differences in the transcription of *SPP1* and *DKK-1* could facilitate prostate cancer metastasis to bone. Osteonectin (secreted protein, acidic and rich cystein [*SPARC*]) was also upregulated by FGF-8b in the PC-3 cells. Osteonectin is associated with aggressive tumor growth and it has been previously shown to promote prostate cancer metastasis to bone [De et al., 2003], although results concerning its metastatic role are somewhat conflicting [De et al., 2003; Wong et al., 2008].

Directional actions of FGFs and compartment-specific location of FGF receptors have an important role in maintaining prostate homeostasis, mainly based on FGF-7 and FGF-10 signaling from stromal cells to epithelial FGFR2b [Jin et al., 2004; Kwabi-Addo et al., 2004]. Disruption of this homeostasis at various points leads to prostate carcinogenesis and tumor progression [Acevedo et al., 2007, 2009; Memarzadeh et al., 2007; Li et al., 2008]. Upregulation of FGFR1 [Acevedo et al., 2007] and FGFR4 and downregulation of FGFR2 [Feng et al., 1997; Jin et al., 2003] have been associated with prostate cancer progression in experimental models and in clinical material [Valve et al., 2001; Sahadevan et al., 2007]. Increased expression of FGF-9 which signals from epithelial/tumor cells to stroma [Jin et al., 2004] has recently been reported to be associated with prostate cancer progression and bone metastases [Li et al., 2008]. In this respect the effects of FGF-8b and FGF-9 resemble each other and it will be interesting to study whether their signaling pathways overlap or interact with each other. Our present and previous results provide evidence that FGF-8b is another epithelium/tumor cell to stroma directed FGF that markedly contributes to disruption of FGF/FGFR maintained prostate homeostasis and prostate cancer progression.

In summary, in this study we showed that ectopic FGF-8b increased the growth of PC-3 prostate cancer cells in vitro, and in vivo in sc and orthotopic prostate tumors in nude mice. FGF-8b also induced a rich network of sinusoidal capillaries in prostate tumors and favored the hematogenic spread of cancer cells. Microarray and RT-qPCR analyses revealed patterns of induction and repression of a number of genes associated with FGF-8b overexpression in PC-3 cells and orthotopic tumors. The upregulated transcripts included several genes that are associated with proliferation and angiogenesis. The downregulated genes were associated with differentiation or cell death. In addition, FGF-8b-responsive genes included that for osteopontin, *DKK-1* and other genes previously shown to be involved in bone metastasis of prostate cancer. The identification of an FGF-8b-responsive gene expression signature in prostate cancer may help in understanding the mechanisms of prostate cancer progression and may provide targets in its treatment.

ACKNOWLEDGMENTS

We thank Soili Jussila, Jani Seppänen and Seija Lindqvist for their excellent technical assistance, Dr. Markku Kallajoki (Department of Pathology) for expert help in histological analyses and Dr. Jorma Määttä for comments and a critical review of the manuscript. Genolyze Ltd (Turku, Finland) is acknowledged for irreplaceable assistance in analysis of the tumor array data. This work was supported by grants from the Academy of Finland (P.L.H. and K.P.), the Finnish Cancer Societies and the Sigrid Jusélius Foundation (P.L.H.), the Southwestern Finnish Cancer Societies (M.P.V. and J.T.) and the Finnish Cultural Foundation (M.P.V.), and European Union 6th Framework contract LSHC-CT-2004-503011 (K.P.).

REFERENCES

Acevedo VD, Gangula RD, Freeman KW, Li R, Zhang Y, Wang F, Ayala GE, Peterson LE, Ittmann M, Spencer DM. 2007. Inducible FGFR-1 activation leads to irreversible prostate adenocarcinoma and an epithelial-to mesenchymal transition. Cancer Cell 12(6):559–571.

Acevedo VD, Ittmann M, Spencer DM. 2009. Paths of FGFR-driven tumorigenesis. Cell Cycle 8(4):580–588.

Aragon-Ching JB, Dahut WL. 2008. The role of angiogenesis inhibitors in prostate cancer. Cancer J 14:20–25.

Cao R, Brakenhielm E, Pawliuk R, Wariaro D, Post MJ, Wahlberg E, Leboulch P, Cao Y. 2003. Angiogenic synergism, vascular stability and improvement of hind-limb ischemia by a combination of PDGF-BB and FGF-2. Nat Med 9:604–613.

Chirgwin JM, Przybyla AE, MacDonald RJ, Rutter WJ. 1979. Isolation of biologically active ribonucleic acid from sources enriched in ribonuclease. Biochemistry 18:5294–5299.

Dailey LD, Ambrosetti D, Mansukhani A, Basilico C. 2005. Mechanisms underlying differential responses to FGF signaling. Cytokine Growth Factor Rev 16:233–247.

De S, Chen J, Narizhneva NV, Heston W, Brainard J, Sage EH, Byzova TV. 2003. Molecular pathway for cancer metastasis to bone. J Biol Chem 278: 39044–39050.

Dennis G, Jr., Sherman BT, Hosack DA, Yang J, Gao W, Lane HC, Lempicki RA. 2003. DAVID: Database for Annotation, Visualization, and Integrated Discovery. Genome Biol 4:P3.

Doll JA, Reiher FK, Crawford SE, Pins MR, Campbell SC, Bouck NP. 2001. Thrombospondin-1, vascular endothelial growth factor and fibroblast growth factor-2 are key functional regulators of angiogenesis in the prostate. Prostate 49:293–305.

Dorkin TJ, Robinson MC, Marsh C, Bjartell A, Neal DE, Leung HY. 1999. FGF8 over-expression in prostate cancer is associated with decreased patient survival and persists in androgen independent disease. Oncogene 18: 2755–2761.

Dube JY, Chapdelaine P, Trahan PL, Deperthes D, Frenette G, Tremblay RR. 1998. Abundant cysteine-rich protein-1 is localized in the stromal compartment of the human prostate. Arch Androl 40:109–115.

Feng S, Wang F, Matsubara A, Kan M, McKeehan WL. 1997. Fibroblast growth factor receptor 2 limits and receptor 1 accelerates tumorigenity of prostate epithelial cells. Cancer Res 57:5369–5378.

Freeman KW, Gangula RD, Welm BE, Ozen M, Foster BA, Rosen JM, Ittmann M, Greenberg NM, Spencer DM. 2003. Conditional activation of fibroblast growth factor receptor (FGFR)1, but not FGFR2, in prostate cancer cells leads to increased osteopontin induction, extracellular signal-regulated kinase activation, and in vivo proliferation. Cancer Res 63:6237–6243.

Ghosh AK, Shankar DB, Shackleford GM, Wu K, T'Ang A, Miller GJ, Zheng J, Roy-Burman P. 1996. Molecular cloning and characterization of human FGF8 alternative messenger RNA forms. Cell Growth Differ 7:1425–1434.

Gnanapragasam VJ, Robson CN, Neal DE, Leung HY. 2002. Regulation of FGF8 expression by the androgen receptor in human prostate cancer. Oncogene 21:5069–5080.

Gnanapragasam VJ, Robinson MC, Marsh C, Robson CN, Hamdy FC, Leung HY. 2003. FGF8 isoform b expression in human prostate cancer. Br J Cancer 88:1432–1438.

Hall CL, Bafico A, Dai J, Aaronson SA, Keller ET. 2005. Prostate cancer cells promote osteoblastic bone metastases through Wnts. Cancer Res 65:7554–7560.

Heer R, Douglas D, Mathers ME, Robson CN, Leung HY. 2004. Fibroblast growth factor 17 is over-expressed in human prostate cancer. J Pathol 204: 578–586.

Hotte SJ, Winquist EW, Stitt L, Wilson SM, Chambers AF. 2002. Plasma osteopontin: Associations with survival and metastasis to bone in men with hormone-refractory prostate carcinoma. Cancer 95:506–512.

Huss WJ, Barrios RJ, Foster BA, Greenberg NM. 2003. Differential expression of specific FGF ligand and receptor isoforms during angiogenesis associated with prostate cancer progression. Prostate 54:8–16.

Janik P, Briand P, Hartmann NR. 1975. The effect of estrone-progesterone treatment on cell proliferation kinetics of hormone-dependent GR mouse mammary tumors. Cancer Res 35:3698–3704.

Jendraschak E, Sage EH. 1996. Regulation of angiogenesis by SPARC and angiostatin: Implications for tumor cell biology. Semin Cancer Biol 7:139–146.

Jin C, McKeehan K, Guo W, Jauma M, Ittman M, Foster B, Greenberg NM, McKeehan WL, Wang F. 2003. Cooperation between ectopic FGFR1 and depression of FGFR2 in induction of prostatic intraepithelial neoplasia in the mouse prostate. Cancer Res 63:8784–8790.

Jin C, Wang F, Wu X, Yu C, Luo Y, McKeehan WL. 2004. Directionally specific paracrine communication mediated by epithelial FGF9 stromal FGFR3 in two-compartment premalignant prostate tumors. Cancer Res 64:4555–4562.

Kawata H, Kamiakito T, Takayashiki N, Tanaka A. 2006. Vitamin D3 suppresses the androgen-stimulated growth of mouse mammary carcinoma SC-3 cells by transcriptional repression of fibroblast growth factor 8. J Cell Physiol 207:793–799.

Kerr K, Afshari C, Bennett L, Bushel P, Martinez J, Walker N, Churchill G. 2002. Statistical analysis of a gene expression microarray experiment with replication. Stat Sinica 12:203–217.

Khodavirdi AC, Song Z, Yang S, Zhong C, Wang S, Wu H, Pritchard C, Nelson PS, Roy-Burman P. 2006. Increased expression of osteopontin contributes to the progression of prostate cancer. Cancer Res 66:883–888.

Kostourou V, Robinson SP, Cartwright JE, Whitley GS. 2002. Dimethylarginine dimethylaminohydrolase I enhances tumour growth and angiogenesis. Br J Cancer 87:673–680.

Kostourou V, Robinson SP, Whitley GS, Griffiths JR. 2003. Effects of overexpression of dimethylarginine dimethylaminohydrolase on tumor angiogenesis assessed by susceptibility magnetic resonance imaging. Cancer Res 63:4960–4966.

Krishnan AV, Peehl DM, Feldman D. 2003. The role of vitamin D in prostate cancer. Recent Results Cancer Res 164:205–221.

Kwabi-Addo B, Ozen M, Ittmann M. 2004. The role of fibroblast growth factors and their receptors in prostate cancer. Endocr Relat Cancer 11:709–724.

Li ZG, Mathew P, Yang J, Starbuck MW, Zurita AJ, Liu J, Sikes C, Multani AS, Efstathiou E, Lopez A, Wang J, Fanning TV, Prieto VG, Kundra V, Vazquez ES, Troncoso P, Raymond AK, Logothetis CJ, Lin SH, Maity S, Navone NM. 2008. Androgen receptor-negative human prostate cancer cells induce osteogenesis in mice through FGF9-mediated mechanisms. J Clin Invest 118(8):2697–2710.

London CA, Sekhon HS, Arora V, Stein DA, Iversen PL, Devi GR. 2003. A novel antisense inhibitor of MMP-9 attenuates angiogenesis, human prostate cancer cell invasion and tumorigenicity. Cancer Gene Ther 10: 823–832.

MacArthur CA, Lawshe A, Shankar DB, Heikinheimo M, Shackleford GM. 1995. FGF-8 isoforms differ in NIH3T3 cell transforming potential. Cell Growth Differ 6:817–825.

Mattila MM, Harkonen PL. 2007. Role of fibroblast growth factor 8 in growth and progression of hormonal cancer. Cytokine Growth Factor Rev 18:257–266.

Mattila MM, Ruohola JK, Valve EM, Tasanen MJ, Seppanen JA, Harkonen PL. 2001. FGF-8b increases angiogenic capacity and tumor growth of androgen-regulated S115 breast cancer cells. Oncogene 20:2791–2804.

Memarzadeh S, Xin L, Mulholland DJ, Mansukhani A, Wu H, Teitell MA, Witte ON. 2007. Enhanced paracrine FGF10 expression promotes formation of multifocal prostate adenocarcinoma and an increase in epithelial androgen receptor. Cancer Cell 12(6):572–585.

Nurmi J, Lilja H, Ylikoski A. 2000. Time-resolved fluorometry in end-point and real-time PCR quantification of nucleic acids. Luminescence 15:381–388.

Olsen SK, Li JY, Bromleigh C, Eliseenkova AV, Ibrahimi OA, Lao Z, Zhang F, Linhardt RJ, Joyner AL, Mohammadi M. 2006. Structural basis by which alternative splicing modulates the organizer activity of FGF8 in the brain. Genes Dev 20:185–198.

Ornitz DM, Xu J, Colvin JS, McEwen DG, MacArthur CA, Coulier F, Gao G, Goldfarb M. 1996. Receptor specificity of the fibroblast growth factor family. J Biol Chem 271:15292–15297.

Parkin DM, Bray FI, Devesa SS. 2001. Cancer burden in the year 2000. The global picture. Eur J Cancer 37 (Suppl 8): S4–S66.

Pepper MS. 2001. Role of the matrix metalloproteinase and plasminogen activator-plasmin systems in angiogenesis. Arterioscler Thromb Vasc Biol 21:1104–1117.

Powers CJ, McLeskey SW, Wellstein A. 2000. Fibroblast growth factors, their receptors and signaling. Endocr Relat Cancer 7:165–197.

Presta M, Dell'Era P, Mitola S, Moroni E, Ronca R, Rusnati M. 2005. Fibroblast growth factor/fibroblast growth factor receptor system in angiogenesis. Cytokine Growth Factor Rev 16:159–178.

Pucci-Minafra I, Cancemi P, Albanese NN, Di Cara G, Marabeti MR, Marrazzo A, Minafra S. 2008. New protein clustering of breast cancer tissue proteomics using actin content as a cellularity indicator. J Proteome Res 7:1412–1418.

Rudra-Ganguly N, Zheng J, Hoang AT, Roy-Burman P. 1998. Downregulation of human FGF8 activity by antisense constructs in murine fibroblastic and human prostatic carcinoma cell systems. Oncogene 16:1487–1492.

Ruohola JK, Valve EM, Vainikka S, Alitalo K, Harkonen PL. 1995. Androgen and fibroblast growth factor (FGF) regulation of FGF receptors in S115 mouse mammary tumor cells. Endocrinology 136:2179–2188.

Ruohola JK, Viitanen TP, Valve EM, Seppanen JA, Loponen NT, Keskitalo JJ, Lakkakorpi PT, Harkonen PL. 2001. Enhanced invasion and tumor growth of fibroblast growth factor 8b-overexpressing MCF-7 human breast cancer cells. Cancer Res 61:4229–4237.

Sahadevan K, Darby S, Leung HY, Mathers ME, Robson CN, Gnanapragasam VJ. 2007. Selective overexpression of fibroblast growth factor receptors 1 and 4 in clinical prostate cancer. J Pathol 213(1):82–90.

Salcedo R, Ponce ML, Young HA, Wasserman K, Ward JM, Kleinman HK, Oppenheim JJ, Murphy WJ. 2000. Human endothelial cells express CCR2 and respond to MCP-1: Direct role of MCP-1 in angiogenesis and tumor progression. Blood 96:34–40.

Salcedo R, Young HA, Ponce ML, Ward JM, Kleinman HK, Murphy WJ, Oppenheim JJ. 2001. Eotaxin (CCL11) induces in vivo angiogenic responses by human CCR3+ endothelial cells. J Immunol 166:7571–7578.

Saucier C, Khoury H, Lai KM, Peschard P, Dankort D, Naujokas MA, Holash J, Yancopoulos GD, Muller WJ, Pawson T, Park M. 2004. The Shc adaptor protein is critical for VEGF induction by Met/HGF and ErbB2 receptors and for early onset of tumor angiogenesis. Proc Natl Acad Sci USA 101:2345–2350.

Siren MJ, Vainiomaki M, Vaananen K, Harkonen P. 2004. alpha-Trinositol inhibits FGF-stimulated growth of smooth muscle and breast cancer cells. Biochem Biophys Res Commun 325:691–697.

Song Z, Powell WC, Kasahara N, van Bokhoven A, Miller GJ, Roy-Burman P. 2000. The effect of fibroblast growth factor 8, isoform b, on the biology of prostate carcinoma cells and their interaction with stromal cells. Cancer Res 60:6730–6736.

Song Z, Wu X, Powell WC, Cardiff RD, Cohen MB, Tin RT, Matusik RJ, Miller GJ, Roy-Burman P. 2002. Fibroblast growth factor 8 isoform B overexpression in prostate epithelium: A new mouse model for prostatic intraepithelial neoplasia. Cancer Res 62:5096–5105.

Stoica GE, Kuo A, Powers C, Bowden ET, Sale EB, Riegel AT, Wellstein A. 2002. Midkine binds to anaplastic lymphoma kinase (ALK) and acts as a growth factor for different cell types. J Biol Chem 277:35990–35998.

Tanaka A, Miyamoto K, Minamino N, Takeda M, Sato B, Matsuo H, Matsumoto K. 1992. Cloning and characterization of an androgen-induced growth factor essential for the androgen-dependent growth of mouse mammary carcinoma cells. Proc Natl Acad Sci USA 89:8928–8932.

Tanaka A, Furuya A, Yamasaki M, Hanai N, Kuriki K, Kamiakito T, Kobayashi Y, Yoshida H, Koike M, Fukayama M. 1998. High frequency of fibroblast growth factor (FGF) 8 expression in clinical prostate cancers and breast tissues, immunohistochemically demonstrated by a newly established neutralizing monoclonal antibody against FGF 8. Cancer Res 58:2053–2056.

Tuomela JM, Valta MP, Vaananen K, Harkonen PL. 2008. Alendronate decreases orthotopic PC-3 prostate tumor growth and metastasis to prostate-draining lymph nodes in nude mice. BMC Cancer 8:81.

Udayakumar TS, Nagle RB, Bowden GT. 2004. Fibroblast growth factor-1 transcriptionally induces membrane type-1 matrix metalloproteinase expression in prostate carcinoma cell line. Prostate 58:66–75.

Vaananen RM, Rissanen M, Kauko O, Junnila S, Vaisanen V, Nurmi J, Alanen K, Nurmi M, Pettersson K. 2008. Quantitative real-time RT-PCR assay for PCA3. Clin Biochem 41:103–108.

Valta MP, Hentunen T, Qu Q, Valve EM, Harjula A, Seppanen JA, Vaananen HK, Harkonen PL. 2006. Regulation of osteoblast differentiation: A novel function for fibroblast growth factor 8. Endocrinology 147:2171–2182.

Valta MP, Tuomela J, Bjartell A, Valve E, Vaananen HK, Harkonen P. 2008. FGF-8 is involved in bone metastasis of prostate cancer. Int J Cancer 123:22–31.

Valve EM, Nevalainen MT, Nurmi MJ, Laato MK, Martikainen PM, Harkonen PL. 2001. Increased expression of FGF-8 isoforms and FGF receptors in human premalignant prostatic intraepithelial neoplasia lesions and prostate cancer. Lab Invest 81:815–826.

Wang Q, Stamp GW, Powell S, Abel P, Laniado M, Mahony C, Lalani EN, Waxman J. 1999. Correlation between androgen receptor expression and FGF8 mRNA levels in patients with prostate cancer and benign prostatic hypertrophy. J Clin Pathol 52:29–34.

West AF, O'Donnell M, Charlton RG, Neal DE, Leung HY. 2001. Correlation of vascular endothelial growth factor expression with fibroblast growth factor-8 expression and clinico-pathologic parameters in human prostate cancer. Br J Cancer 85:576–583.

Wilt TJ, Thompson IM. 2006. Clinically localized prostate cancer. BMJ 333: 1102–1106.

Wong SY, Crowley D, Bronson RT, Hynes RO. 2008. Analyses of the role of endogenous SPARC in mouse models of prostate and breast cancer. Clin Exp Metastasis 25:109–118.

Yan G, Fukabori Y, McBride G, Nikolaropolous S, McKeehan WL. 1993. Exon switching and activation of stromal and embryonic fibroblast growth factor (FGF)-FGF receptor genes in prostate epithelial cells accompany stromal independence and malignancy. Mol Cell Biol 13:4513–4522.

Zhang Y, Zhang J, Lin Y, Lan Y, Lin C, Xuan JW, Shen MM, McKeehan WL, Greenberg NM, Wang F. 2008. Role of epithelial cell fibroblast growth factor receptor substrate 2alpha in prostate development regeneration and tumorigenesis. Development 135(4):775–784.